communications

Individual Nanometer Hole–Particle Pairs for Surface-Enhanced Raman Scattering**

Hong Wei, Ulf Håkanson, Zhilin Yang, Fredrik Höök,* and Hongxing Xu*

Metal nanostructures have been widely explored for their extraordinary optical properties which are caused by surface plasmon resonances (SPRs).[1] Surface-plasmon-based analytical techniques have been well developed, of which surface-enhanced Raman scattering (SERS)[2–5] and SPR-based biochemical sensing are two of the most important applications.[6] For SPR sensors, the physical principle of their sensitivity is the change of the SPR wavelength owing to the adsorption of analytes.[7–9] SPR excitation has also been shown to generate enhanced optical fields near metal nanostructures, which is the main mechanism for SERS.[10] As a consequence, SERS shows greatly enhanced molecular sensitivity and since it also can provide unique vibrational fingerprints of molecules, it is becoming a useful spectroscopic tool in biochemistry and biomedicine.[6,11] For instance, SERS was used for quantitative glucose detection, which might help diabetes patients to monitor their glucose levels.[12] More recently, SERS was employed in the study of cancer diagnostics.[13]

Metal nanoparticles are today important substrates for studying SERS- and SPR-based biochemical sensing.[14–17] Strong SERS enhancement up to single-molecule sensitivity can be obtained in aggregates of metal nanoparticles because of the strong electromagnetic coupling between neighboring nanoparticles.[18–20] Other interesting types of nanostructure are nanometer holes in opaque gold or silver films. Sparked by the discovery of the extraordinary optical transmission through sub-wavelength hole arrays,[21] nanohole structures in metal films have attracted increasing scientific interest for their extraordinary optical properties,[22,23] including selective transmissions,[24] beaming light,[25] and large electromagnetic field enhancement.[26] In addition, plasmonic-sensing characteristics of both multiple[27] and single[28] nanometer holes have been well studied to confirm the localized character of the hole plasmon, and more recently quasi-3D structures composed of nanoholes and nanodisks were also studied for quantitative multispectral biosensing.[29] Periodic nanohole arrays have additionally been used as SERS substrates owing to their large electromagnetic field enhancement and since the surface plasmon excitation wavelength can be tuned by varying the periodicity of the nanohole arrays.[30] However, nanometer holes in thin metal films do not provide as strong SERS enhancements as observed for aggregates of metal nanoparticles. For single nanometer holes, SERS enhancement was even weaker than hole arrays owing to the lack of coupling between holes.[30] To our knowledge, no SERS experiment of single holes has been reported to date.

Herein we report the use of self-assembly colloidal lithography[28,31] for the fabrication of nanometer-sized apertures in thin gold films on SiO$_2$ and investigate their compatibility with SERS through the binding of rhodamine 6G and malachite green isothiocyanate. Specifically, through a material-specific surface modification of the gold film by using thiol-PEG, site-selective binding of poly-L-lysine to the SiO$_2$ bottom of the holes is shown to provide a template for directed nanoparticle binding to the bottom of the holes. In this way, we were able to compare the enhancement of the SERS signals for individual holes, individual particles, and for combined hole–particle systems. Supported by a theoretical analysis, the latter system is shown to provide an enhancement factor even higher than that obtained through conventional metal-nanoparticle aggregation, which was so far the most commonly used method to achieve extraordinary SERS enhancement[18–20] proven to be compatible with single-molecule sensitivity.[14,18] More strikingly, the volume for extraordinary SERS enhancement in the hole–particle system can be one order of magnitude larger than for particle aggregates. Besides high SERS enhancement within a volume significantly larger than that of aggregated spherical nanoparticles, the system presented herein also allows a plasmonically active nanoparticle to be located in close proximity to a plasmonically active nanohole through site-selective binding of the nanoparticle to a substrate, as schematically illustrated in Figure 1a. Hence, the self assembly system is generic in the sense that it is compatible also with chemistries that prevent nanoparticle aggregation through either short- or long-range repulsion. The extension of this work to biosensor applications based on novel surface modifications involving lipid-based surface modifications[27,32] is discussed.

In the nanohole sample fabrication using colloidal lithography,[28,31] polystyrene particles (white-sulfate latex, IDC) of diameter 140 nm were first adsorbed on a clean cover glass through electrostatic interaction. The distance between

[*] H. Wei, Dr. Z. Yang, Prof. H. Xu
Laboratory of Soft Matter Physics
Beijing National Laboratory for Condensed Matter Physics, and
Institute of Physics, Chinese Academy of Sciences
PO Box 603-146
Beijing, 100190 (P.R. China)
Fax: (+86) 1082649228
E-mail: hxxu@aphy.iphy.ac.cn

Dr. U. Håkanson, Prof. H. Xu, Prof. F. Höök+
Division of Solid State Physics/The Nanometer Consortium
Lund University, PO Box 118
Lund, S-221 00 (Sweden)
E-mail: fredrik.hook@ftf.lth.se

[+] Present address: Department of Physics
Chalmers University of Technology Göteborg, 41296 (Sweden)

☐ Supporting Information is available on the WWW under http://www.small-journal.com or from the author.
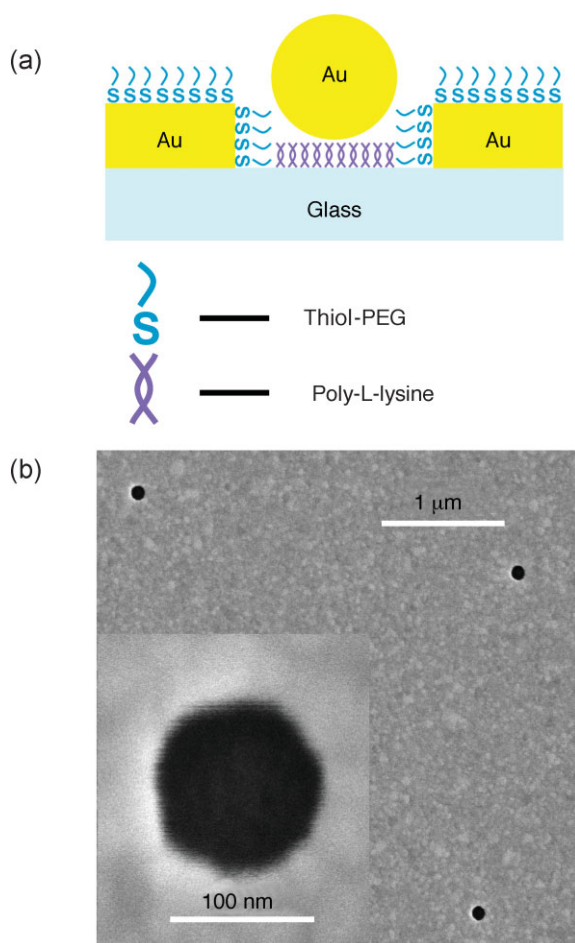
Figure 1. a) Schematic illustration of the system studied. b) Representative SEM image of the nanoholes in the 55-nm-thick gold film. The inset shows a higher-magnification image of a single hole.

particles was controlled by particle concentration and adsorption time. After oxygen-plasma etching, a 1-nm-thick chromium film was thermally evaporated onto the substrate followed by evaporation of a 55-nm-thick gold film. The particles were then removed with tape resulting in a 55nm-thick gold film containing nanoholes with diameter of about 120 nm and separation of about 3 μm. Figure 1b shows a scanning electron microscopy (SEM) image of the nanohole sample.

To control spontaneous binding of gold nanoparticles to the bottom of the nanoholes, the samples were modified by means of material-specific chemistry. First, the sample was cleaned in TL1 (30% NH_3 + 30% H_2O_2 + H_2O 1:1:5 $v/v/v$ at ≈80 °C for ≈10 min). The cleaned sample was soaked in a 1 mM solution of SH-PEG-OH (MW 3000, Rapp Polymere) in ethanol for ≈1–2 h at about 40 °C, rinsed with ethanol, and dried with N_2 gas. This provides a chemically inert modification of the gold film, but leaves the SiO_2 bottom of the holes free for subsequent modifications.[32] The SiO_2 bottom of the holes were then modified by immersing the sample in 0.01% poly-L-lysine (MW 70000–150000, Sigma–Aldrich) for ≈1–2 h at room temperature, followed by rinsing with water, and drying with N_2 gas. The chemical modifications were

confirmed by a using quartz crystal microbalance with dissipation (QCM-D) monitoring (not shown), as described previously.[32] The treatment results in a gold film covered by SH-PEG-OH, whereas the bottom of the nanoholes is covered with poly-L-lysine (see Figure 1a), since the thiol group can be strongly bonded to the gold atom and the carboxy group in poly-L-lysine can be bonded to the Si atoms on the glass surface. Finally, the sample was soaked in a gold colloid solution (particle diameter 80 nm or 100 nm, BBInternational) for about 12 h, and rinsed thoroughly with Milli-Q H_2O. As verified by SEM, this resulted in efficient formation of hole–particle pairs, although the absolute position of the particles varied (see further below).

For SERS measurements, rhodamine 6G (R6G, Sigma) and malachite green isothiocyanate (MGITC, Invitrogen) were employed as probe molecules. Since the absorption peak of MGITC molecules is near the incident laser wavelength, additional resonance Raman enhancement can be expected, in contrast to the R6G case. The nanohole samples with adsorbed gold nanoparticles were immersed in 100 μM solutions of R6G (in water) or MGITC (in ethanol) for 3 h and dried with N_2 gas. By marking the samples with a UV-lithography-defined coordinate system, the same hole–particle pairs identified in the SEM could be investigated later in the optical microscope of the Raman system. The topological details of the nanometer hole–particle pairs could readily be determined by SEM, and the obtained information was used as input for theoretical calculations (see below). For comparison, SERS measurements were performed, under the same experimental conditions, on single gold nanoparticles on a glass substrate and on single nanoholes in the gold film.

The plasmonic properties of the metal nanostructures were investigated by acquiring dark-field (DF) scattering spectra. Figure 2 shows typical DF scattering spectra of a single hole, a single gold particle, and a hole–particle pair. The peak position for a single nanohole is at about 640 nm, as shown in Figure 2a, and the corresponding SEM image of the hole is shown to the right. For a gold nanoparticle with a diameter of about 80 nm, the maximum scattering is at about 570 nm. Interestingly, the scattering spectrum of the nanometer hole–particle pair shows two peaks (560 nm and 660 nm), which correspond to two different plasmon modes. The two modes can be explained with a plasmon hybridization model,[33] in which the plasmon response of metal nanostructures is treated as the interaction of plasmons from the elementary geometries. In this hole–particle pair system, the plasmon property is the result of the interaction between plasmons supported by both the nanoparticle and the nanohole. This interaction may result in two new plasmon modes different from either the nanoparticle or the nanohole modes.

For MGITC molecules, only weak SERS signals could be detected from single gold nanoparticles attached on glass substrates and from single nanoholes in a gold film. As shown in Figures 3a and 3b, these systems give comparable Raman signals. Notably, for a gold film without nanoholes, the same SERS spectra with similar intensities were obtained as in the case of single holes. Hence, the contribution from the gold film dominates the total SERS enhancement. When, however, hole–particle pairs were analyzed, the SERS intensity of
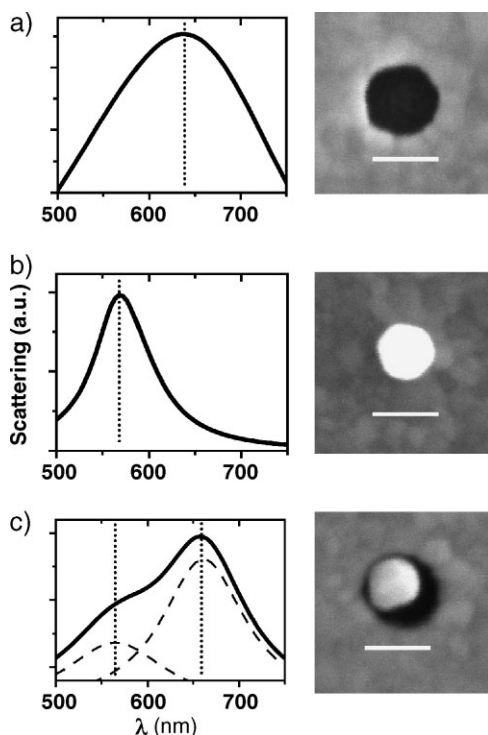
Figure 2. Dark-field scattering spectra of a) a single nanohole in a gold film, b) a single gold nanoparticle on a glass substrate, and c) a single nanometer hole–particle pair. Representative SEM images of these nanostructures are shown on the right. The scale bars in the SEM images represent 100 nm. The spectra shown are the result Lorentzian correction. The original data can be found in the Supporting Information.
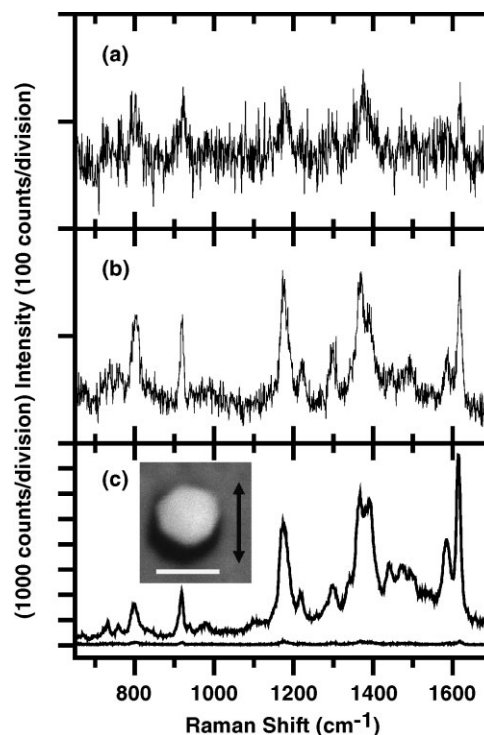

Figure 3. SERS spectra of MGITC detected from a) a single gold nanoparticle on a glass substrate, b) a single nanohole in a gold film, and c) a single nanometer hole–particle pair. For comparison, the spectrum in (b) is also plotted in (c). The corresponding hole–particle pair is shown in the inset. The scale bare is 100 nm. The arrow shows the polarization of incident laser light.

MGITC molecules was shown to be enhanced by almost two orders of magnitude. This can be seen in Figure 3c, where the hole–particle pair gives a strong SERS spectrum of MGITC molecules with the same characteristics as reported earlier.[34] As a comparison, the spectrum of a single hole is also shown in Figure 3c. Analysis of the obtained SERS signals shows that the difference in intensity is as much as 60 times larger at Raman peak of about $1615\,cm^{-1}$ for the hole–particle pair than for the gold film (with or without nanohole). This clearly shows that even if the gold film contributes to the total SERS signals of the hole–particle system, it is the hole–particle coupling that dominates the field enhancement. The intensity of the hole–particle pair is about 100 times larger than the SERS intensity of the single gold nanoparticle.

Furthermore, our experiments show that the SERS enhancement varies for hole–particle pairs with different separations between the nanohole edges and the nanoparticles. Figure 4 shows three examples of SERS measurements on R6G molecules adsorbed onto hole–particle pairs. In Figure 4a, there is no detectable R6G SERS signal for this particular hole–particle pair, whereas in Figure 4b, the SERS intensity is detectable but still rather weak. The reason for this observation is attributed to the fact that the separations between the hole edges and the particles are fairly large for the system shown in Figures 4a and 4b. Hence, no strong plasmon coupling between the hole and the particle can occur, resulting

in nondetectable or weak SERS. In contrast, in Figure 4c, in which case the particle–hole separation distance is much smaller (see inset of Figure 4c), the SERS enhancement is a factor of about 10 higher. Interestingly, no SERS signals were observed for R6G molecules adsorbed on either single gold nanoparticles supported on glass substrates or on gold films (with or without nanoholes). This thus illustrates the potential of the system for SERS analysis, and it is emphasized that these results were obtained despite the fact that the gold film was chemically modified with a chemically inert monolayer of PEG with a (collapsed) thickness of about 3 nm. Hence, since the metal nanoparticles were directed to the bottom of the holes by spontaneous adsorption to poly-L-lysine-modified SiO_2, the system will be fully compatible with the analysis of molecular modifications of metal nanoparticles, which prevent or complicate nanoparticle aggregation.
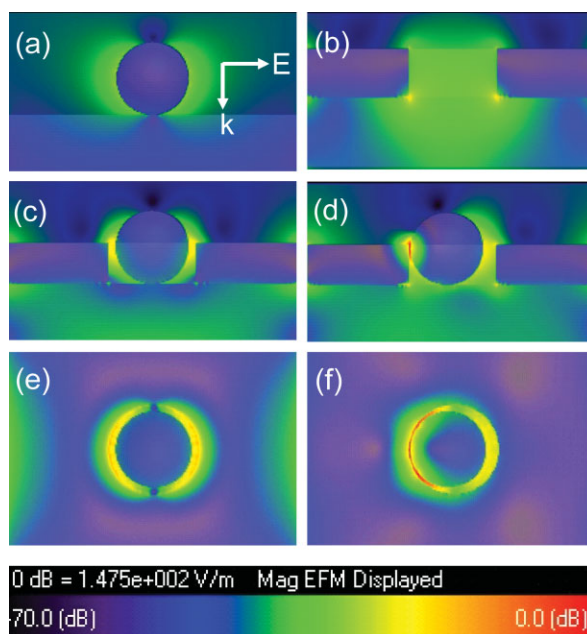
The experimental observations were further compared with three-dimensional finite difference time domain (FDTD)[35] simulations. To simulate the detailed hole–particle nanostructure accurately, the Yee cell size used in our calculation was set to be $0.5 \times 0.5 \times 0.5\,nm^3$, which was much smaller than the size of relevant nanoparticle features. The number of the periods of the incident sinusoidal plane wave was set to 10, in order to guarantee the calculation convergence, which could be judged by checking whether near-zone electric field values have reached a steady state. The amplitude of the sinusoidal plane

© 2008 Wiley-VCH Verlag GmbH & Co. KGaA, Weinheim
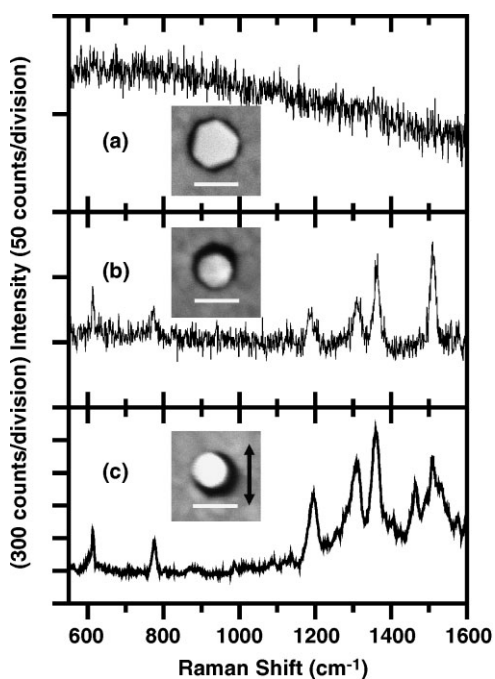
Figure 4. SERS spectra of R6G detected from different hole–particle pairs. All the scale bars in the insets are 100 nm. The polarization of the incident laser is the same for all cases and indicated in the inset of (c).

0 dB = 1.475e+002 V/m   Mag EFM Displayed
-70.0 (dB)   0.0 (dB)

Figure 5. FDTD simulations for a) a single gold nanoparticle of diameter 100 nm on a glass substrate, b) a single nanometer hole of diameter 120 nm in a 55-nm-thick gold film, c) a nanometer hole–particle pair with the particle at the center of the hole, and d) close to the edge of the hole; e) and f) are the top views of (c) and (d), respectively. The arrows in (a) show the directions of incident wave vector k and the electric field E.

wave was set to be $1\,\mathrm{V\,m^{-1}}$ in the calculation, and the excitation wavelength was 632.8 nm. The dielectric constants of gold were obtained from the literature.[36]

Figure 5a shows the calculated field distribution of a single gold nanoparticle with 100-nm diameter on a glass substrate. The maximum electric field enhancement is just about 7.5 times larger than the incident light, which corresponds to a SERS-enhancement factor, fourth power of the field enhancement E^4, of 3.1×10^3. For single nanometer holes of 120-nm diameter in a 55-nm-thick gold film, the maximum enhancement is only a factor of 5% stronger than that of single gold nanoparticles. However, the maximum SERS enhancement for either single holes or single particles is still on the same order. It can also be seen that the maximum enhanced volume is located at the corner of the bottom of the hole inside the glass substrate, as shown in Figure 5b. Since this region is not available for molecular binding, it cannot contribute to SERS. For nanometer hole–particle pairs, the hole–particle coupling effect gives rise to a strong SERS enhancement. It should be pointed out, though, that the enhancement strongly depends on where the particle is located. As seen in Figure 5c, in which the particle is located at the center of the hole, the SERS enhancement is about a factor of 5 stronger (1.6×10^4) than that of a single particle or hole. In contrast, when the particle is moved towards the rim of the hole, the SERS enhancement increases dramatically in the area where the separation between the particle and the hole is smallest. For a separation of 3 nm, which roughly corresponds to the collapsed thickness of the monolayer of PEG, the maximum field enhancement is as high as 147, which corresponds to more than 8 orders of SERS enhancement ($147^4 \approx 4.7 \times 10^8$). Interest-

ingly, the generalized Mie theory[20] gives a maximum field enhancement of 121 for two spherical gold nanoparticles with a diameter of 100 nm separated by 3 nm, assuming the same laser excitation as above. This corresponds to a SERS enhancement of $\approx 2.1 \times 10^8$, that is, about two times lower than for the particle — hole case. Even more importantly, the volume defined by an enhancement over 10^8 is shown to be about 20 times larger for the particle–hole system than for the particle–particle system. In the hole–particle system, the same directions of the curvatures of the particle and the hole edge allow the volume of the cavity within which the fields of the plasmonically active nanostructures will couple to be significantly larger than in the case of two spherical particles with opposite curvatures. Furthermore, when the two particle surfaces are moved away from the symmetry axis, the distance of the gap increases very fast and eliminates the electromagnetic enhancement quickly. This is the reason why a 20-times-larger "hot" volume for SERS can be obtained in the new system. This is considered a significant improvement for SERS analysis.

In summary, the simulations performed qualitatively confirm the experimental observations, and will, together with further optimization of particle and hole dimensions, aid the development of chemical modifications that will allow the system to be applied for SERS analysis of various molecular entities not easily approached by using particle aggregation. Although two 100-nm Au particles separated by 3 nm provide a similar field enhancement, the advantages of this system are that 1) the volume within which the field is extraordinarily high is up to 20 times larger than that provided by aggregated nanoparticles, and 2) the system relies on specific binding of

nanoparticles to a chemically modified substrate in close proximity to a plasmonic active hole. The latter component makes the concept particularly interesting for studies of biomolecular systems in general, and for studies of lipid bilayers in particular. First, lipid bilayers have a thickness of about 5 nm, which is close to the preferred distances for sufficient SERS enhancement in this system. Second, both lipid bilayers and lipid vesicles can be directed either to the bottom of the plasmonically active holes[27,32] or to the gold film.[37] When combined with site-selective binding of metal nanoparticles, through for example DNA hybridization,[38] this is expected to provide SERS analysis both of various lipids as well as lipid membrane constituents, such as membrane proteins, which currently constitute the class of proteins to which a majority of drugs are directed. The latter are often aromatic, and thus of high relevance of SERS.

Experimental Section

Optical spectroscopy was performed with a confocal-fiber-coupled Raman microscope system (InduRAM, HORIBA Jobin Yvon), consisting of an Olympus BX41 microscope equipped with an XY scanning stage (minimum scanning step 100 nm) and Z motorization (1 μm step^{-1}), and a fiber-coupled rack-mounted spectrometer equipped with a TE air cooled 1024×256 CCD detector. Raman signals were obtained through a $100 \times$ objective (NA 0.9) by using a He–Ne laser at the wavelength of 632.8 nm in a backscattering configuration. The laser power on the sample was 0.7 mW, and the exposure time for SERS measurements was 10 s. For DF scattering spectra, unpolarized white light from a 100-W halogen lamp was sent to the sample through a dark-field condenser (NA = 1.20–1.44). Scattered light was collected by the $100 \times$ objective.

[1] U. Kreibig, M. Vollmer, *Optical properties of Metal Clusters*, Springer, New York **1995**.
[2] M. Moskovits, *Rev. Mod. Phys.* **1985**, *57*, 783–826.
[3] K. Kneipp, H. Kneipp, I. Itzkan, R. R. Dasari, M. S. Feld, *Chem. Rev.* **1999**, *99*, 2957–2975.
[4] Z. Q. Tian, *J. Raman Spectrosc.* **2005**, *36*, 466–470.
[5] G. A. Baker, D. S. Moore, *Anal. Bioanal. Chem.* **2005**, *382*, 1751–1770.
[6] K. A. Willets, R. P. Van Duyne, *Annu. Rev. Phys. Chem.* **2007**, *58*, 267–297.
[7] N. Nath, A. Chilkoti, *Anal. Chem.* **2002**, *74*, 504–509.
[8] J. J. Mock, D. R. Smith, S. Schultz, *Nano Lett.* **2003**, *3*, 485–491.
[9] G. Raschke, S. Kowarik, T. Franzl, C. Sonnichsen, T. A. Klar, J. Feldmann, A. Nichtl, K. Kurzinger, *Nano Lett.* **2003**, *3*, 935–938.
[10] G. C. Schatz, M. A. Young, R. P. Van Duyne, *Top. Appl. Phys.* **2006**, *103*, 19–45.

[11] K. Kneipp, H. Kneipp, I. Itzkan, R. R. Dasari, M. S. Feld, *J. Phys. Condens. Mat.* **2002**, *14*, R597–R624.
[12] K. E. Shafer-Peltier, C. L. Haynes, M. R. Glucksberg, R. P. Van Duyne, *J. Am. Chem. Soc.* **2003**, *125*, 588–593.
[13] X. H. Huang, I. H. El-Sayed, W. Qian, M. A. El-Sayed, *Nano Lett.* **2007**, *7*, 1591–1597.
[14] K. Kneipp, Y. Wang, H. Kneipp, L. T. Perelman, I. Itzkan, R. Dasari, M. S. Feld, *Phys. Rev. Lett.* **1997**, *78*, 1667–1670.
[15] C. E. Talley, J. B. Jackson, C. Oubre, N. K. Grady, C. W. Hollars, S. M. Lane, T. R. Huser, P. Nordlander, N. J. Halas, *Nano Lett.* **2005**, *5*, 1569–1574.
[16] A. J. Haes, R. P. Van Duyne, *J. Am. Chem. Soc.* **2002**, *124*, 10596–10604.
[17] C. Sonnichsen, B. M. Reinhard, J. Liphardt, A. P. Alivisatos, *Nat. Biotechnol.* **2005**, *23*, 741–745.
[18] H. X. Xu, E. J. Bjerneld, M. Kall, L. Borjesson, *Phys. Rev. Lett.* **1999**, *83*, 4357–4360.
[19] A. M. Michaels, J. Jiang, L. Brus, *J. Phys. Chem. B* **2000**, *104*, 11965–11971.
[20] H. X. Xu, J. Aizpurua, M. Kall, P. Apell, *Phys. Rev. E* **2000**, *62*, 4318–4324.
[21] T. W. Ebbesen, H. J. Lezec, H. F. Ghaemi, T. Thio, P. A. Wolff, *Nature* **1998**, *391*, 667–669.
[22] C. Genet, T. W. Ebbesen, *Nature* **2007**, *445*, 39–46.
[23] F. J. Garcia de Abajo, *Rev. Mod. Phys.* **2007**, *79*, 1267–1290.
[24] K. J. K. Koerkamp, S. Enoch, F. B. Segerink, N. F. van Hulst, L. Kuipers, *Phys. Rev. Lett.* **2004**, *92*, 183901.
[25] H. J. Lezec, A. Degiron, E. Devau x, R. A. Linke, L. Martin-Moreno, F. J. Garcia-Vidal, T. W. Ebbesen, *Science* **2002**, *297*, 820–822.
[26] L. Salomon, F. D. Grillot, A. V. Zayats, F. de Fornel, *Phys. Rev. Lett.* **2001**, *86*, 1110–1113.
[27] A. Dahlin, M. Zach, T. Rindzevicius, M. Kall, D. S. Sutherland, F. Hook, *J. Am. Chem. Soc.* **2005**, *127*, 5043–5048.
[28] T. Rindzevicius, Y. Alaverdyan, A. Dahlin, F. Hook, D. S. Sutherland, M. Kall, *Nano Lett.* **2005**, *5*, 2335–2339.
[29] M. E. Stewart, N. H. Mack, V. Malyarchuk, J. Soares, T. W. Lee, S. K. Gray, R. G. Nuzzo, J. A. Rogers, *Proc. Natl. Acad. Sci. USA* **2006**, *103*, 17143–17148.
[30] A. G. Brolo, E. Arctander, R. Gordon, B. Leathem, K. L. Kavanagh, *Nano Lett.* **2004**, *4*, 2015–2018.
[31] P. Hanarp, D. S. Sutherland, J. Gold, B. Kasemo, *Colloids Surf. A* **2003**, *214*, 23–36.
[32] A. Dahlin, M. Jonsson, F. Hook, *Adv. Mater.* **2008**, *20*, 1436–1442.
[33] E. Prodan, C. Radloff, N. J. Halas, P. Nordlander, *Science* **2003**, *302*, 419–422.
[34] K. F. Domke, D. Zhang, B. Pettinger, *J. Am. Chem. Soc.* **2006**, *128*, 14721–14727.
[35] K. S. Kunz, R. J. Luebbers, *The Finite Difference Time Domain Method for Electromagnetics*, CRC, Boca Raton, FL **1993**.
[36] E. D. Palik, *Handbook of Optical Constants of Solids*, Academic, New York **1985**.
[37] S. Svedhem, I. Pfeiffer, C. Larsson, C. Wingren, C. Borrebaeck, F. Hook, *ChemBioChem.* **2003**, *4*, 339–343.
[38] B. Stadler, H. H. Solak, S. Frerker, K. Bonroy, F. Frederix, J. Voros, H. M. Grandin, *Nanotechnology* **2007**, *18*, 155306.